

ARTICLE

Longitudinal profiling of human blood transcriptome in healthy and lupus pregnancy

Seunghee Hong^{1,2,3*}, Romain Banchereau^{3,4*}, Bat-Sheva L. Maslow^{5*} , Marta M. Guerra⁶ , Jacob Cardenas³, Jeanine Baisch^{1,2,3}, D. Ware Branch^{7,8}, T. Flint Porter^{7,8}, Allen Sawitzke⁷, Carl A. Laskin⁹ , Jill P. Buyon¹⁰, Joan Merrill¹¹, Lisa R. Sammaritano^{6,12}, Michelle Petri¹³ , Elizabeth Gatewood³, Alma-Martina Cepika³, Marina Ohouo^{1,2,3} , Gerlinde Obermoser³, Esperanza Anguiano³ , Tae Whan Kim^{1,2,3}, John Nulsen¹⁴, Djamel Nehar-Belaid⁵ , Derek Blankenship³, Jacob Turner³ , Jacques Banchereau^{5**} , Jane E. Salmon^{6,12**}, and Virginia Pascual^{1,2,3**} 

Systemic lupus erythematosus carries an increased risk of pregnancy complications, including preeclampsia and fetal adverse outcomes. To identify the underlying molecular mechanisms, we longitudinally profiled the blood transcriptome of 92 lupus patients and 43 healthy women during pregnancy and postpartum and performed multicolor flow cytometry in a subset of them. We also profiled 25 healthy women undergoing assisted reproductive technology to monitor transcriptional changes around embryo implantation. Sustained down-regulation of multiple immune signatures, including interferon and plasma cells, was observed during healthy pregnancy. These changes appeared early after embryo implantation and were mirrored in uncomplicated lupus pregnancies. Patients with preeclampsia displayed early up-regulation of neutrophil signatures that correlated with expansion of immature neutrophils. Lupus pregnancies with fetal complications carried the highest interferon and plasma cell signatures as well as activated CD4⁺ T cell counts. Thus, blood immunomonitoring reveals that both healthy and uncomplicated lupus pregnancies exhibit early and sustained transcriptional modulation of lupus-related signatures, and a lack thereof associates with adverse outcomes.

Introduction

Systemic lupus erythematosus (SLE), an autoimmune disease characterized by excess type I IFN, predominantly affects women and often presents during their childbearing years. SLE patients are at increased risk of pregnancy complications, including preeclampsia (PE), fetal or neonatal death, and fetal morbidity from growth restriction and preterm delivery (Clowse et al., 2008; Bundhun et al., 2017). These adverse outcomes affect over one fifth of SLE pregnancies (Buyon et al., 2015). Progress was made in characterizing clinical factors and circulating antiangiogenic factors as predictors of poor pregnancy outcomes, but identification of patients destined for complications remains challenging (Buyon et al., 2015).

Pregnancy requires tolerance of fetal alloantigens encoded by paternal genes. A variety of factors at the maternal–fetal interface protect the fetus from maternal immune responses, including expression of HLA-G (Hunt and Geraghty, 2005),

expansion and local accumulation of maternal T regulatory cells (Jiang et al., 2014), immunosuppressive trophoblast-derived exosomes, and epigenetic modifications of decidual stromal cells that limit effector T cell trafficking (PrabhuDas et al., 2015). Absence of these regulatory mechanisms leads to inflammation and trophoblast dysfunction with ensuing placental insufficiency, poor fetal growth, preterm birth, and in some cases, the maternal syndrome of PE.

Experimental models of pregnancy in lupus-like conditions implicate inflammation at the maternal–fetal interface as an essential factor in fetal death and growth restriction (Girardi et al., 2003; Berman et al., 2005). Activation of complement, recruitment of neutrophils, and production of proinflammatory cytokines and antiangiogenic factors are drivers of poor placental development in mice treated with antiphospholipid antibodies and in nonautoimmune models of PE (Girardi et al.,

¹Druker Institute for Children’s Health, Weill Cornell Medicine, New York, NY; ²Department of Pediatrics, Weill Cornell Medicine, New York, NY; ³Baylor Institute for Immunology Research, Dallas, TX; ⁴Oncology Biomarker Development, Genentech, South San Francisco, CA; ⁵The Jackson Laboratory for Genomic Medicine, Farmington, CT; ⁶Department of Medicine and Program in Inflammation and Autoimmunity, Hospital for Special Surgery, New York, NY; ⁷University of Utah Health Sciences Center, Salt Lake City, UT; ⁸Intermountain Healthcare, Salt Lake City, UT; ⁹Mount Sinai Hospital and the University of Toronto, Toronto, Ontario, Canada; ¹⁰New York University School of Medicine, New York, NY; ¹¹Oklahoma Medical Research Foundation, Oklahoma City, OK; ¹²Department of Medicine, Weill Cornell Medicine, New York, NY; ¹³Johns Hopkins University School of Medicine, Baltimore, MD; ¹⁴University of Connecticut School of Medicine, Farmington, CT.

*S. Hong, R. Banchereau, and B-S.L. Maslow contributed equally to this paper; **J. Banchereau, J. Salmon and V. Pascual contributed equally to this paper; Correspondence to Virginia Pascual: vip2021@med.cornell.edu and Jane E. Salmon: salmonj@hss.edu; V. Pascual’s present address is Weill Cornell Medicine, New York, NY.

© 2019 Hong et al. This article is distributed under the terms of an Attribution–Noncommercial–Share Alike–No Mirror Sites license for the first six months after the publication date (see <http://www.rupress.org/terms>). After six months it is available under a Creative Commons License (Attribution–Noncommercial–Share Alike 4.0 International license, as described at <https://creativecommons.org/licenses/by-nc-sa/4.0/>).

2003, 2006; Gelber et al., 2015), and there is evidence that these mechanisms also contribute to adverse outcomes in human pregnancies (Shamonki et al., 2007; Cohen et al., 2011; Kim et al., 2016). In addition, increased neutrophil numbers and neutrophil extracellular traps (NETs) infiltrating placental intervillous spaces associate with inflammatory, vascular changes in patients with SLE and PE (Marder et al., 2016). Neutrophils are a source of interferogenic nucleic acids (Caielli et al., 2016; Lood et al., 2016) and IFN α has been shown in vitro to prevent stabilization of endothelial cells and thus potentially contribute to PE (Andrade et al., 2015). Furthermore, IFN β lowers the threshold for inflammatory-driven cytokine release systemically and at reproductive sites (Cappelletti et al., 2017).

Transcriptional biomarkers have been used to study placental tissue, uterine endothelial cells, and the endometrium during healthy pregnancy (Gack et al., 2005; Schmidt et al., 2005; Kitaya et al., 2007; Yockey and Iwasaki, 2018). Measuring these biomarkers, however, requires invasive procedures with associated risks. Blood transcriptional profiling has been widely reported in SLE (Baechler et al., 2003; Bennett et al., 2003; Chaussabel et al., 2008; Banchereau et al., 2016) but never before in SLE pregnancy.

Blood profiling during late stages of pregnancy identified PE-associated cell proliferation, differentiation, and apoptosis-related transcriptional changes (Textoris et al., 2013). We hypothesized that a similar approach applied from early pregnancy might identify SLE patients at high risk for complications. Accordingly, we evaluated the blood transcriptome in individuals from the PROMISSE (Predictors of pRegnancy Outcome: bio-Markers In antiphospholipid antibody Syndrome and Systemic Lupus Erythematosus) study. PROMISSE is the largest multicenter, multiethnic, and multiracial study to prospectively assess clinical and laboratory predictors of adverse outcomes in SLE patients with inactive or mild/moderate disease activity at conception. We profiled the blood transcriptome of SLE patients and healthy pregnant women by microarray and conducted multicolor flow cytometry in a subset of them. To identify the earliest molecular changes associated with pregnancy onset, the blood transcriptome of healthy women undergoing assisted reproductive technologies (ARTs) was profiled before and after embryo implantation by RNA sequencing.

Both in healthy and noncomplicated SLE pregnancies, as well as during the peri-implantation period, we observed a striking transcriptional modulation of immune networks associated with SLE pathogenesis. Incomplete down-regulation of several of these pathways was associated with SLE pregnancy complications, supporting their potentially pathogenic role at the maternal–fetal interface.

Results

Cohorts and study design

Longitudinal blood transcriptional profiles were applied to samples from the prospective, multicenter, observational PROMISSE study. Among PROMISSE patients, adverse outcomes occurred in 19.0% of pregnancies, including fetal (4%) or neonatal (1%) death, preterm delivery <36 wk because of

placental insufficiency (9%), and small-for-gestational-age neonate (10%; Buyon et al., 2015). Our study included 92 SLE pregnant, 43 healthy pregnant (H-P), 20 SLE nonpregnant (SLE-NP), and 34 healthy nonpregnant (H-NP) women. For pregnant subjects, the average gestational age at recruitment was 12.2 weeks. Samples drawn at specific time points (P1: <16 wk of gestation [WG]; P2: 16–23 WG; P3: 24–31 WG; P4: 32–40 WG; and between 8 and 20 wk postpartum [PP]) were used for microarray analysis (Fig. 1 A). SLE-pregnant patients were further stratified according to pregnancy outcomes: no complications (NC; $n = 46$), PE ($n = 24$), and other fetal-related complications in the absence of PE (OC; $n = 22$). There were no differences in hydroxychloroquine use among patient groups. For patients receiving steroids, the mean daily dose of prednisone was <10 mg. Unequal sample size distribution of patients in P3 and P4 was due to complication-related premature delivery in the SLE-OC and PE groups (Fig. 1 A).

In addition, we studied 25 subjects undergoing ART by blood RNA sequencing (RNA-seq; Fig. 1 B). Successful pregnancy rate for this cohort was 80% (20/25). There were no significant demographic differences between those who conceived compared with those who did not (Table S1). Blood was drawn on the day of embryo transfer, in the midluteal phase (4–5 d after embryo transfer), on the day of pregnancy test (9 d after embryo transfer), and during the first trimester of pregnancy (P0: 4–6 wk after embryo transfer), when applicable.

Blood transcriptome dynamics during healthy pregnancy

We first characterized the blood transcriptional changes elicited over time during healthy pregnancy. To identify differentially expressed transcripts (DETs) at various time points, disease status, and/or complications while accounting for individual variation and missing data, we developed a linear mixed model that included both fixed and random effects. Using H-NP women as baseline controls, 9,576 DETs were identified. Hierarchical clustering revealed prominent transcriptional down-regulation, in line with the highly dynamic immunomodulatory features associated with pregnancy (Mor et al., 2017; Fig. 2 A). Principal component analysis highlighted a gradual shift in signatures away from H-NP from <16 WG that stabilized by 16–23 WG through delivery. The healthy PP signature only partially returned to H-NP baseline, indicating that sustained blood transcriptional changes remain detectable several weeks after delivery (Fig. 2 B).

To interpret these signatures, we leveraged a framework of 260 coexpression modules specifically designed for whole-blood transcriptome analysis, which can detect alterations in both leukocyte frequency and population-intrinsic transcriptional signaling (Chaussabel and Baldwin, 2014). To simplify data interpretation, we depict modules M1–7 (97 out of 260), which display the most conserved coexpression behavior across independent datasets. The global module fingerprint of pregnancy, which combines profiles from four time points compared with H-NP, revealed up-regulation of neutrophil (M5.15), myeloid inflammation (M3.2, M4.2), and erythropoiesis (M2.3, M3.1, M6.18) signatures (Fig. 2, C and D). Conversely, antiviral and lymphocyte-related pathways were downregulated, including

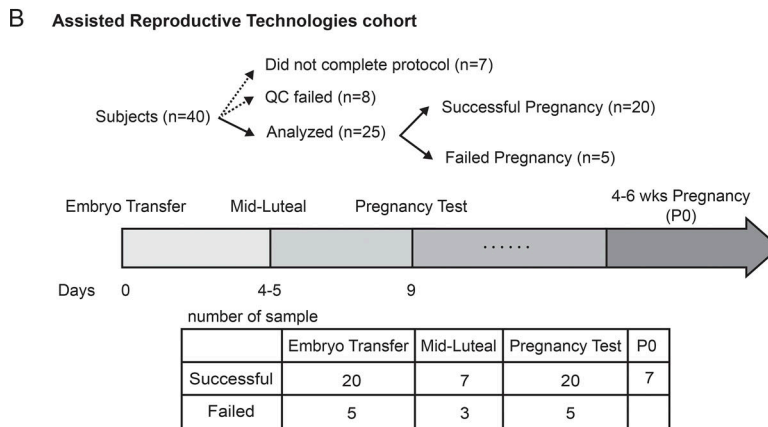
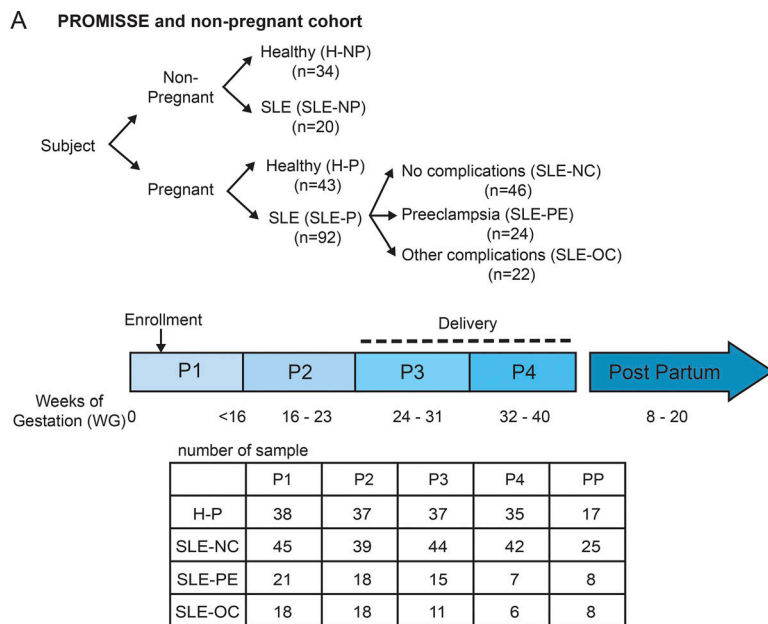


Figure 1. PROMISSE study design. (A) 92 SLE pregnant (SLE-P), 43 H-P, 20 SLE-NP, and 34 H-NP females were recruited. Pregnant SLE patients included NC ($n = 46$), PE ($n = 24$), and OC ($n = 22$). Blood was drawn in PAX gene tubes for microarray at specific time points (P1: <16 WG; P2: 16–23 WG; P3: 24–31 WG; P4: 32–40 WG, and between 8 and 20 wk PP). **(B)** Blood from 25 healthy women who underwent ART was analyzed for before and after embryo transfer by RNA-seq. Pregnancy rate for the cohort was 80% (20/25). Samples were taken on the day of the embryo transfer, midluteal, day of the pregnancy test, and P0 (4–6 WG).

modules ascribed to IFN responses (M1.2, M3.4, M5.12), B cells (M4.10), plasma cells (M4.11, M7.7, M7.32), T cells (M4.1, M6.15), and natural killer (NK) cell/cytotoxicity (M3.6, M4.15).

To analyze the evolution of these signatures at each quarter, we used Q-Gen (Turner et al., 2015), a gene-set enrichment approach leveraging QuSAGE (Yaari et al., 2013) that integrates statistics from linear mixed models (Table S2). Significantly altered modules (false discovery rate [FDR]-adjusted $P \leq 0.05$, absolute expression >30% in any comparison) were represented as a heatmap (Fig. 3 A), with the five most significant also represented as a line graph (Fig. 3 B). Increase in erythropoiesis and inflammation was detectable as early as P1, while enrichment in neutrophils appeared at P2. Modulation of these signatures was sustained until delivery and subsequently diminished at PP to levels lower than those of H-NP controls. Down-regulation of IFN response- and lymphoid lineage-related modules was detected as early as P1. To validate these changes during healthy pregnancy, whole-blood FACS analysis was conducted on 11 healthy pregnant individuals, three of whom were also transcriptionally profiled (Table S3). An increase in absolute numbers of circulating neutrophils (granular CD14⁺

CD66b⁺) and a decrease in transitional B cells (CD20⁺ IgD⁺ CD24⁺ CD38²⁺) during pregnancy (P1–4) were detected, suggesting that part of the observed transcriptional changes reflect fluctuations in the frequencies of specific leukocyte subsets (Fig. 3 C and Table S4).

Blood transcriptome association with embryo implantation outcome

To capture early molecular changes associated with pregnancy onset, we monitored the blood transcriptome during embryonic implantation in an independent cohort of 25 age-matched healthy women undergoing ART (Fig. 1 B). Using a mixed model adjusting for subject and time point, combined with Q-Gen analysis incorporating blood modules, early systemic transcriptional changes could be detected at pregnancy onset. Modules that significantly changed at one or more time points compared with their own baseline (embryo transfer) in failed or successful pregnancy are represented as a heatmap (Fig. 4 A). The IFN response increased during the midluteal phase (midluteal vs. embryo transfer; fold change [FC] = 2.16; nominal $P = 0.03$) but was rapidly down-regulated by pregnancy test in

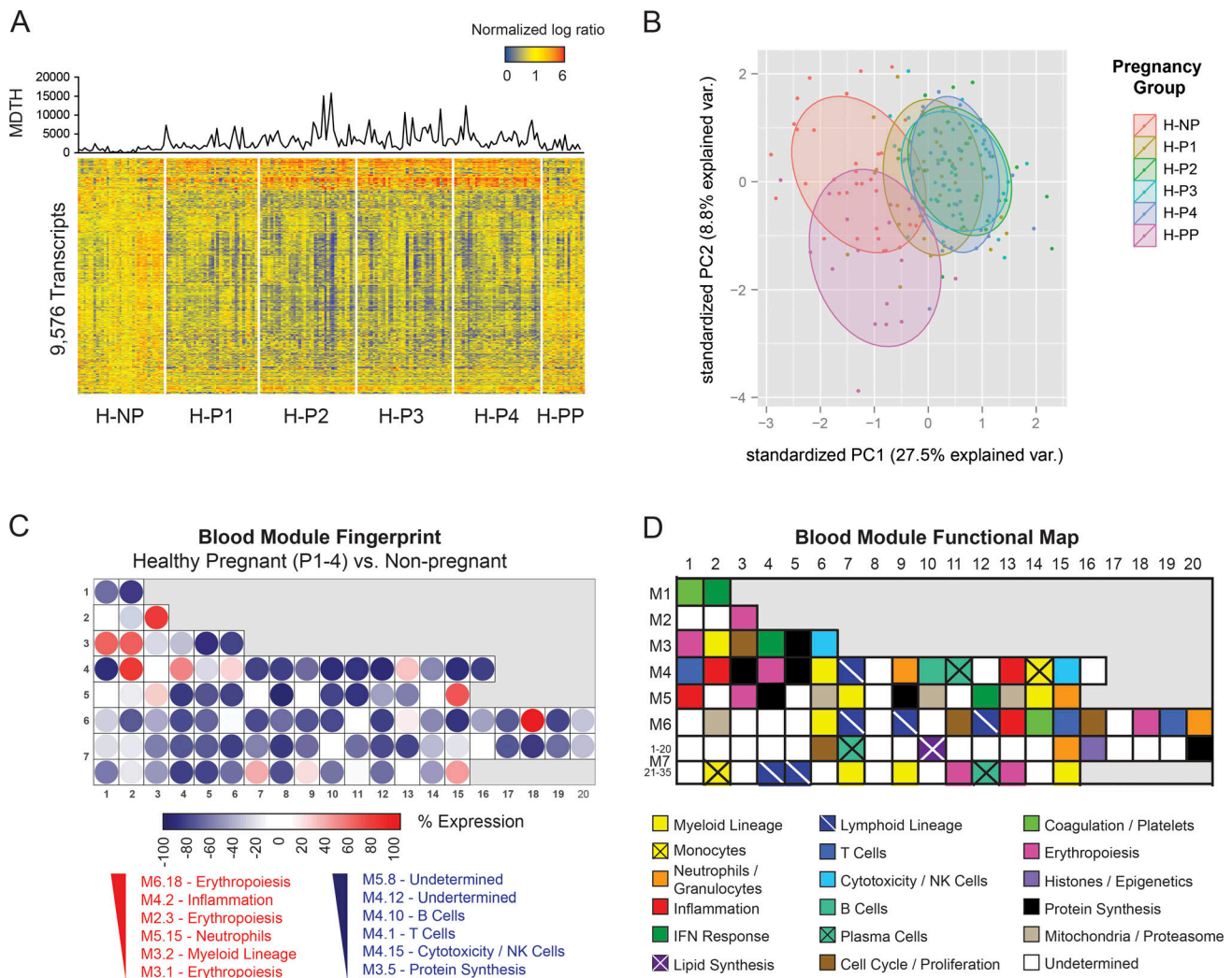


Figure 2. Global blood transcriptome alterations during healthy pregnancy. (A) Hierarchical clustering of the 9,576 DETs between H-P and H-NP individuals. The list of DETs was obtained from the union of all transcripts identified as significantly modulated by the model through contrasts considering each pregnancy time point vs. H-NP (FDR-adjusted $P \leq 0.05$). The line chart represents the molecular distance to health (MDTH) for individual samples, calculated as the sum of absolute FCs ≥ 2 for each transcript. (B) Principal component analysis based on the 9,576 transcripts in A. Dots represent individual samples and color coded by pregnancy group. (C) Blood module fingerprint of healthy pregnancy (P1 to P4, combined) in M1–7. Each dot on the grid represents a module, either overexpressed (red) or underexpressed (blue) as compared with H-NP controls. The intensity of the dots represents the percentage of transcripts from the modules that pass the over- or underexpression threshold. (D) Blood module functional map. PC, principal component; var, variance.

successful pregnancy (pregnancy test vs. embryo transfer; FC = 1.67; nominal $P = 0.04$), while in failed implantations it was further up-regulated at the time of pregnancy test (pregnancy test vs. embryo transfer; FC = 3.14; nominal $P = 0.02$). Conversely, erythropoiesis (M2.3) was down-regulated at midluteal (midluteal vs. embryo transfer; FC = 0.79; nominal $P = 0.05$) but subsequently up-regulated at pregnancy test in successful pregnancies (PO vs. midluteal; FC = 1.5; nominal $P = 0.02$), in contrast to its down-regulation in failed pregnancies (pregnancy test vs. midluteal; FC = 0.62; nominal $P = 0.04$; Fig. 4 B and Table S5). Many IFN-regulated genes were up-regulated in failed pregnancies at the time of pregnancy test (nominal $P \leq 0.05$, FC > 1.25 ; Fig. 4 C). These results demonstrate that some of the significant systemic transcriptional changes in maternal hematopoietic compartments start as early as embryonic implantation. They highlight the down-regulation of major immune

pathways that are linked to SLE pathogenesis, including the IFN response, and suggest that erythropoiesis-related pathways may be linked to pregnancy-induced immune regulation.

Transcriptional fingerprint of noncomplicated SLE pregnancy

To assess the transcriptome of noncomplicated SLE pregnancy (SLE-NC), we compared the signatures of SLE-NP and SLE-NC women with their respective healthy controls using module maps (Fig. 5 A, top and middle). As reported before for adult and pediatric patients (Chiche et al., 2014; Banchereau et al., 2016), SLE-NP displayed several modular differences compared with healthy controls, including increased IFN and neutrophil signatures (M1.2, M3.4, M5.12, and M5.15; Fig. 5 A, top). A plasma cell signature (M4.11) was only mildly increased, likely reflecting the low disease activity in enrolled patients (mean SLE Pregnancy Disease Activity Index [SLEPDAI] score at screening: 2.5;

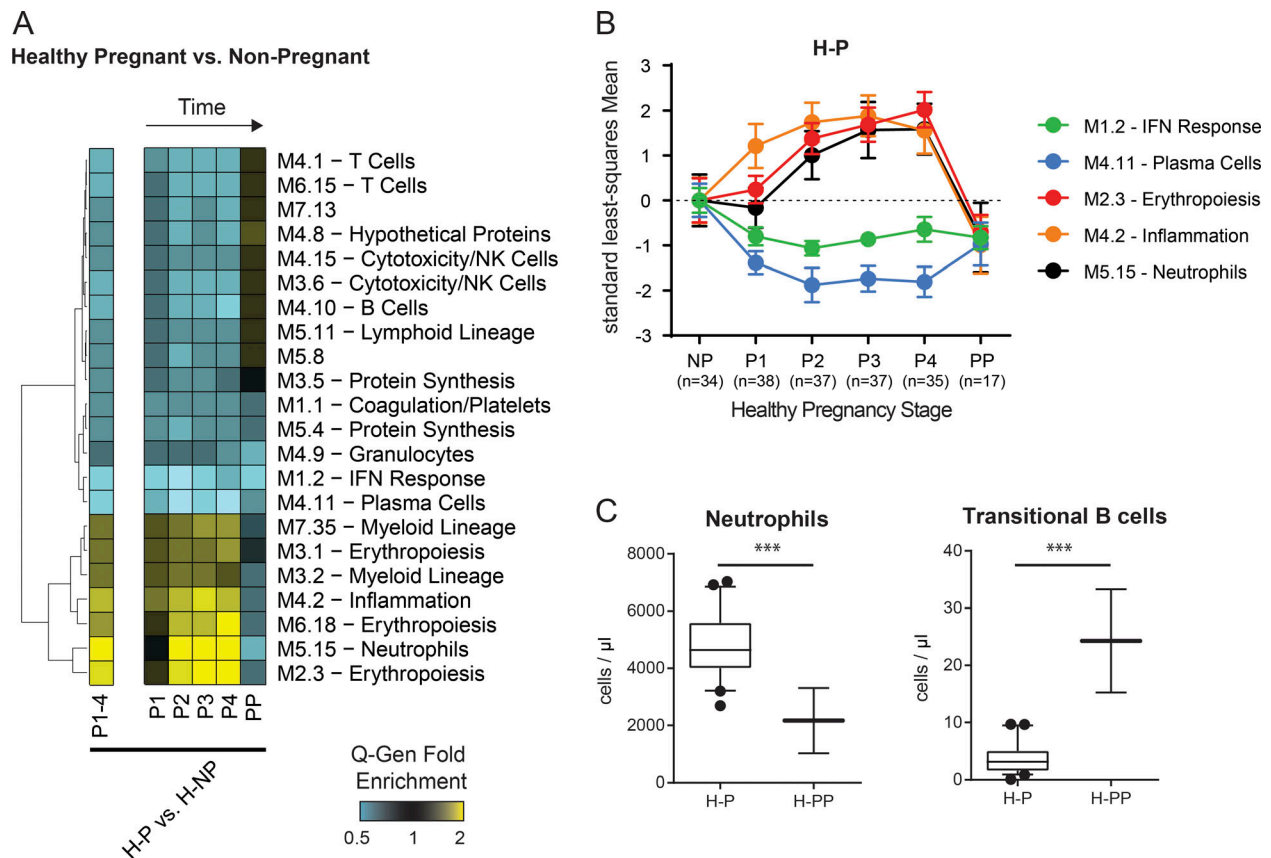


Figure 3. **Increased neutrophil and decreased IFN and plasma cell signatures during healthy pregnancy.** (A) Heatmap representing the Q-Gen fold enrichment for all pregnancy time points combined (H-P, P1–P4) and each individual time point vs. H-NP. Blood modules were used as gene sets. Modules modulated in any comparisons with FDR-adjusted $P \leq 0.05$ and $\geq 30\%$ FC were selected. (B) Line charts representing the standard least-squares mean for inflammation, erythropoiesis, neutrophils, IFN response, and plasma cell modules. Data are normalized to H-NP controls. (C) Box plots representing the absolute numbers of circulating neutrophils (granular CD14⁺ CD66b⁺) and transitional B cells (CD20⁺ IgD⁺ CD24⁺ CD38⁺⁺) during H-P and at PP in flow cytometry analysis. Error bars represent standard deviation. ***, $P < 0.001$.

Table S6). The gene expression signature of SLE-NC compared with H-P controls retained elements of the prototype SLE-NP signature, such as IFN and plasma cell-related transcripts, but included additional up-regulated modules such as cell cycle (M3.3; Fig. 5 A, middle). Myeloid inflammation signatures (M3.2, M4.2, M4.13, M4.14, and M7.27), which were differentially expressed in SLE-NP compared with H-NP, were similarly increased in SLE-NC and H-P (Fig. 2 C). Compared with SLE-NP controls, SLE-NC exhibited remarkable conservation of healthy pregnancy patterns, including down-regulation of all three IFN as well as lymphoid and plasma cell modules and up-regulation of neutrophil and erythropoiesis modules (Fig. 5 A, bottom; and Fig. 2 C). Thus, the transcriptome dynamics of uncomplicated SLE pregnancy mirrors that of healthy pregnancy, but several disease-associated signatures remain dysregulated compared with healthy pregnant controls.

We next compared the profiles of SLE-NC and H-P at each time point and observed 3,138 DETs between the two groups at one or more time points (Fig. 5 B). The largest differences were observed at P2 (1,491 transcripts) and PP (1,252 transcripts). Q-Gen analysis of SLE-NC using the SLE-NP baseline as comparator at each time point confirmed that most elements of the

H-P signature were reproduced over time in SLE-NC (Fig. 5 C). Despite widespread transcriptional down-regulation, the increase in neutrophil, erythropoiesis, and myeloid inflammation modules observed in H-P between P1 and P2 was conserved in SLE-NC. Normalization of the SLE-NP and SLE-NC profiles to those of H-NP confirmed that the most significant modular patterns of H-P were reproduced in SLE-NC (Fig. 5 D). Interestingly, while the IFN response down-regulation in SLE-NC did not reach H-NP or H-P levels, the plasma cell signature steadily decreased below the SLE-NP baseline from P1, reaching levels comparable to H-P by P4 and returning to SLE-NP levels after delivery. These results support that the modulatory effects on major transcriptional networks that take place during healthy pregnancy are conserved in SLE pregnancy. The steady and consistent decrease in plasma cell transcripts below H-NP down to H-P levels suggests that modulation of this pathway is a key element of successful SLE pregnancy.

Transcriptional fingerprints of complicated SLE pregnancy

Up to 19% of SLE pregnancies in the PROMISSE study resulted in either maternal and/or fetal-perinatal complications. This sub-study was enriched in the number of complications by design

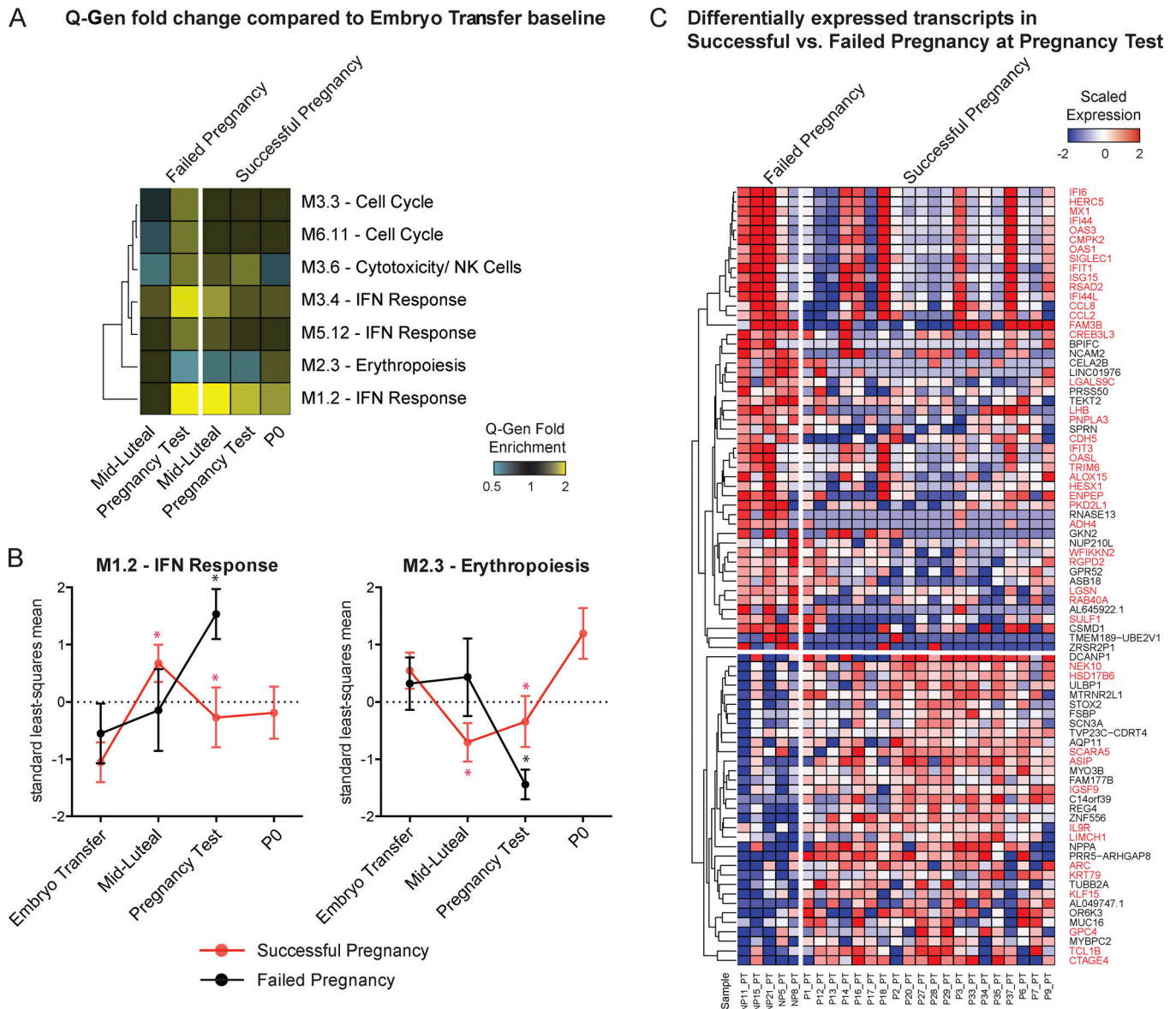


Figure 4. **Decreased IFN signature during successful embryo implantation.** (A) Heatmap representing the Q-Gen fold enrichment for each time point vs. embryo transfer in failed ($n = 5$) and successful ($n = 20$) pregnancies. Blood modules were used as gene sets, and modules changed with nominal $P \leq 0.05$ and $\geq 30\%$ FC were selected and represented. (B) Line chart of the Q-Gen fold enrichment for IFN (M1.2) and erythropoiesis (M2.3) modules for successful or failed pregnant subjects. Significantly modulated time points compared with their own embryo transfer are indicated with asterisks ($P \leq 0.05$). (C) DETs in successful vs. failed pregnancy at pregnancy test (nominal $P \leq 0.05$, $FC > 1.25$) are represented. Genes either in IFN modules or Interferome v2.01 (Rusinova et al., 2013) are highlighted in red.

and included 50% of SLE-PE/OC. Because the pathogenic mechanisms leading to these complications are likely to be different, we classified patients into PE and “complications other than PE” (OC) groups. H-P and SLE-NC women delivered on average at term (39.3 and 38.7 WG, respectively), while delivery time for complicated pregnancies was 30.8 WG (SLE-PE) and 31.5 WG (SLE-OC; Fig. 6 A and Table S6).

To identify maternal blood profiles associated with complications, we compared signatures of SLE-PE or SLE-OC with those of SLE-NC at each time point during pregnancy using a linear model combined with Q-Gen analysis. Significantly altered modules are depicted as a heatmap in Fig. 6 B, and the most

differentially expressed modules among SLE groups are represented as line graphs normalized to H-NP in Fig. 6 C. Higher fold expression of the neutrophil signature was detected in pregnancies destined for PE compared with all other groups at P1 (PE vs. NC; $FC = 1.44$; FDR-adjusted $P < 0.0001$), which supports data from experimental models (Gelber et al., 2015). T cell (M4.1) and B cell (M4.10) signatures were down-regulated in early stages in all pregnancy groups, but more significantly in PE (Fig. 6 C and Fig. S1). In addition, suppression of IFN, cell cycle, and especially plasma cell responses were less pronounced in SLE-OC compared with PE. The dynamic pattern of each differentially expressed module by patient group is represented in Fig. S1.

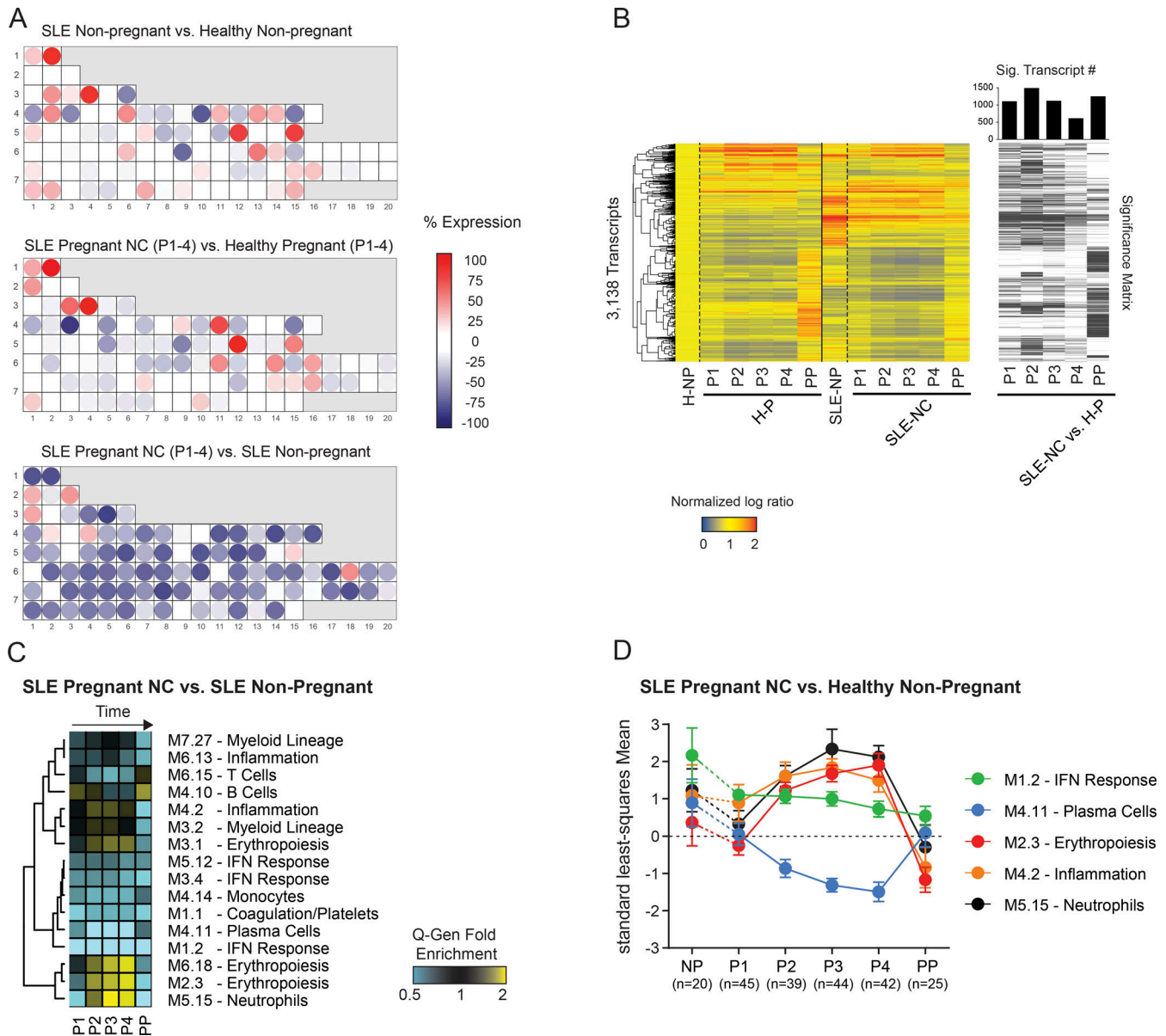


Figure 5. **Blood transcriptome alterations in noncomplicated SLE pregnancy.** (A) Blood module fingerprints of SLE-NP ($n = 20$) vs. H-NP ($n = 34$), SLE pregnant with NC (SLE-NC; $n = 46$) vs. H-P ($n = 43$) and SLE-NC vs. SLE-NP. Each dot on the grid represents a module, either overexpressed (red) or underexpressed (blue) as compared with H-NP controls. The intensity of the dots represents the percentage of transcripts from the modules that pass the over- or underexpression threshold. (B) Hierarchical cluster of 3,138 DETs between SLE-NC and H-P at any time point. Transcript statistics across all comparisons are highlighted in the significance matrix on the right. The number of significant transcripts for each comparison (FDR-adjusted $P \leq 0.05$) is displayed as a bar chart above the matrix. (C) Heatmap representing the blood module Q-Gen fold enrichment for each time point in SLE-NC vs. SLE-NP. Modules with FDR-adjusted $P \leq 0.05$ and 30% FC in at least one condition were selected. (D) Line chart of the standard least-squares mean for inflammation, erythropoiesis, neutrophils, IFN response, and plasma cell modules in SLE-NP and SLE-NC normalized to H-NP controls throughout pregnancy. Sig, significant.

Interestingly, the kinetics of inflammation, myeloid lineage, and especially erythropoiesis transcriptional pathways were conserved in all SLE groups and H-P. These signatures are therefore mostly affected by pregnancy, regardless of health status.

High SLE disease activity at conception is associated with increased risk of pregnancy complications (Clowse et al., 2005; Buyon et al., 2015). In the PROMISSE cohort, disease activity score measured by SLEPDAI was slightly higher at the first time point (P1) in SLE-PE (4.43) compared with SLE-OC (2.86) and SLE-NC (2.35) ($P = 0.026$; Table S6). A second measure of disease

activity, the Physician Global Assessment, was comparable across all groups of patients (Table S6). To confirm that PE signatures were not due to overrepresentation of subjects with high disease activity, we compared PE and OC with NC by a mixed model using the earliest time point (P1) with or without the initial SLEPDAI score as a covariate. Modular maps (Fig. S2) representing Q-Gen FC in gene expression in PE vs. NC and OC vs. NC displayed more significant differences after adjustment for SLEPDAI score. This analysis specifically highlights the increased neutrophil signature (M5.15) in SLE-PE and the

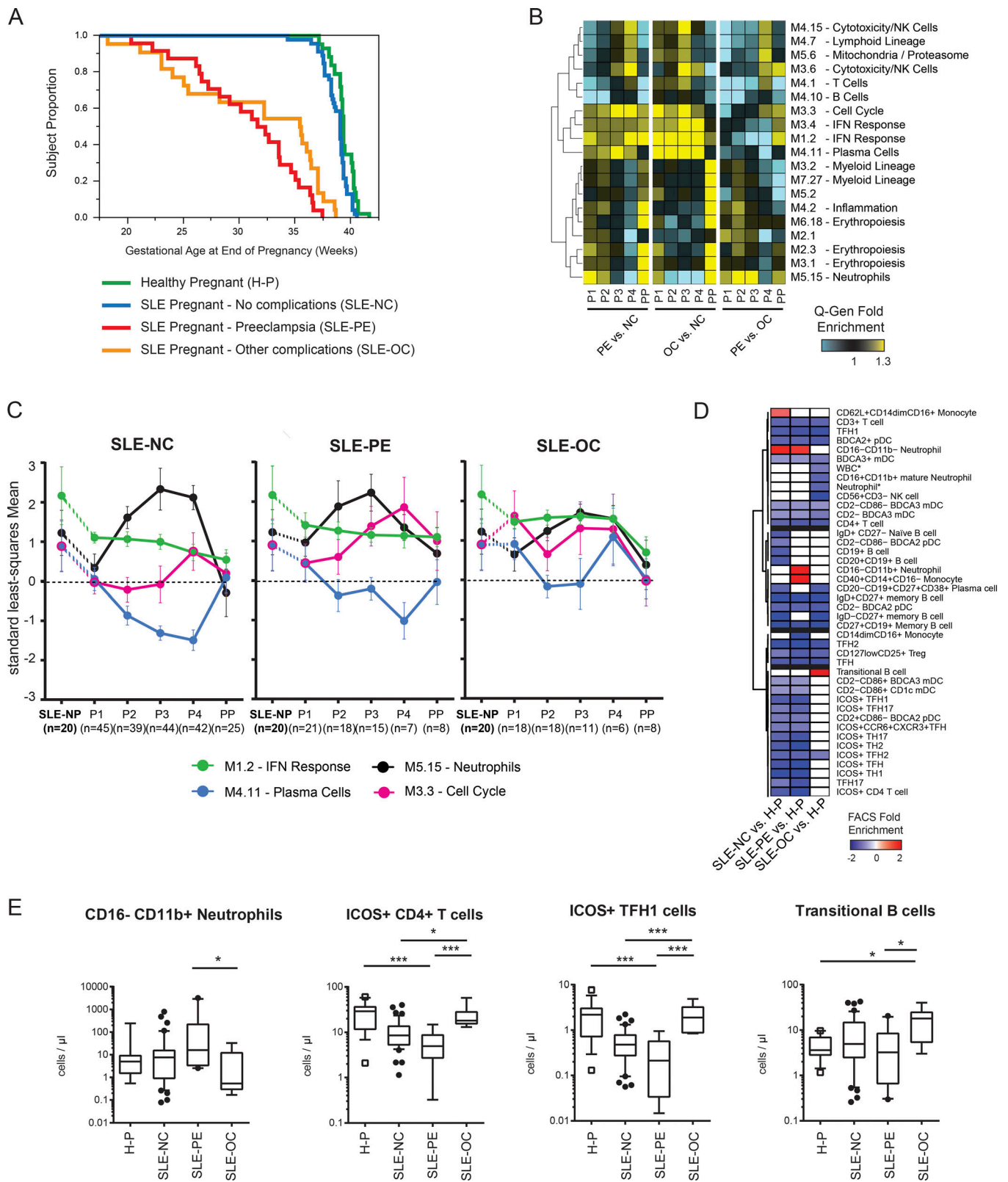


Figure 6. **Blood transcriptome alteration in complicated SLE pregnancy.** (A) Kaplan-Meier curve representing gestational age at the end of pregnancy in H-P ($n = 43$), SLE-NC ($n = 46$), SLE-PE ($n = 24$), and SLE-OC ($n = 22$) cohorts. (B) Heatmap representing the blood module Q-Gen fold enrichment for indicated comparisons at specific time points. Modules with FDR-adjusted $P \leq 0.05$ and $\geq 30\%$ FC in at least one condition were selected. (C) Line chart depicting standard least-squares mean for IFN responses, plasma cells, neutrophils, and cell cycle in SLE-NC, PE, and OC. All values are normalized to H-NP controls. (D) Heatmap representing the normalized fold enrichment in FACS-analyzed leukocyte subsets at P1 and P2 combined. Red represents a statistically significant increase (FDR-adjusted $P \leq 0.05$), blue a statistically significant decrease (FDR-adjusted $P \leq 0.05$), and white a non-statistically significant change. Asterisks

indicate data obtained from complete blood counts. **(E)** Box plot of flow cytometry analysis for a subset of patients (27 SLE-NC, 5 SLE-PE, and 4 SLE-OC) at P1 and P2 combined for immature neutrophils (granular fraction, CD14⁻ CD16⁻ CD11b⁻), ICOS⁺ CD4⁺ T cells, ICOS⁺ CD4⁺ XCR5⁺ Tfh cells, and transitional B cells (CD20⁺ CD38⁺ CD24⁺ CD27⁻). ****, $P < 0.0001$.

increased plasma cell signature (M4.11, M7.7, M7.32) in SLE-OC. In addition, it highlights an up-regulation of erythropoiesis and protein synthesis/degradation pathways (M2.3, M4.5, M6.16) in SLE-OC. These data support that signatures related to SLE-PE/OC were not confounded by higher disease activity. The SLEP-DAI score was measured at baseline and each trimester. Except for baseline, however, it was not obtained simultaneously with samples for transcriptional studies, and therefore it could not be included as a covariate in analyses of later time points.

To complement transcriptomics results, multicolor FACS analysis was performed in a subset of patients (27 SLE-NC, 5 SLE-PE, and 4 SLE-OC) at P1 and P2, when pregnancy complications were not yet clinically apparent. Transcriptional profiles were simultaneously obtained in 10 (28%) of these patients. Among the 84 cell populations/phenotypes assessed, 42 showed significantly altered frequency in any comparison of PE vs. NC, OC vs. NC, and PE vs. OC in a mixed-model analysis (Fig. 6 D and Table S3). PE showed increased frequency of immature neutrophils at this time point (granular fraction, CD14⁻ CD16⁻ CD11b⁻ cells; nominal $P = 0.017$; Fig. 6 E). OC patients displayed increased frequency of activated T cells, as defined by inducible costimulatory molecule (ICOS) expression, both in the total CD4⁺ T cell compartment (nominal $P = 0.038$) as well as within the follicular helper T (Tfh) cell subset (CD4⁺ CXCR5⁺ ICOS⁺; nominal $P = 0.0034$). Within Tfh cells, we detected an expansion of CXCR3⁺ cells (Tfh1; nominal $P = 0.0012$). Within the B cell compartment, transitional B cells (CD20⁺ CD24⁺ CD38²⁺) were significantly expanded in OC (nominal $P = 0.02$). Early expansion of immature neutrophils in PE and activated T cells in OC might underlie the overexpression of neutrophil and T cell signatures observed in these patient groups, respectively (Fig. 6 B). These results suggest that both innate and adaptive arms of immunity are modulated at early stages of SLE pregnancy and that their dysregulation associates with the development of complications. To facilitate access to data and results from our analyses, we generated and formatted results from statistical analysis that can be uploaded into the genBart shiny app in R. In this interactive interface, users can upload our genBart file (downloadable at <http://dx.doi.org/10.17632/hg596dwd6.1>) to view sample information, generate transcriptional heatmaps and module maps, access the mixed model and Q-Gen results of the microarray, browse gene lists driving modular expression, access FACS analysis results, and generate plots for subsets of interest. The interface features are detailed in Fig. S3.

A predictive signature of PE in SLE

Finally, we sought to identify early transcriptional biomarkers that could predict SLE pregnancy-related PE. Machine learning approaches were applied to P1 transcriptional profiles to predict pregnancy outcomes (PE = 21; NC = 45; total = 66) and compared with previously reported laboratory and clinical variables, including lupus anticoagulant, antihypertensive medication use,

Physician Global Assessment score >1, low platelet count, race, and antiangiogenic factors (sFlt1, PlGF, and sFlt1/PlGF; Buyon et al., 2015; Kim et al., 2016). A higher percentage of patients with lupus anticoagulant was present in complicated vs. non-complicated SLE pregnancies, but, likely due to sample size, this variable did not reach significance (25% in PE, 38% in OC, and 9% in NC; Fisher's exact test, $P = 0.08$; Table S6).

We trained the model using 8,201 genes after removing unannotated transcripts and/or selecting one representative for highly correlated transcripts (correlation coefficient >0.7), then performed 10-fold cross-validation on six independent prediction methods using the entire cohort (Fig. 7 A and Table S7). The resulting predictive accuracy on cross-validation was first compared with models using only laboratory/clinical variables, then to models using laboratory/clinical variables combined with transcriptional data. Accuracy of transcriptional prediction ranged from 71.4% to 78.7% (mean accuracy: 74.2%), exceeding that of laboratory/clinical parameters (mean: 67.8%). When transcripts were combined with laboratory/clinical data, their mean accuracy was slightly higher (mean: 75.7%), suggesting that clinical parameters provided additive predictive value to transcriptional data. Receiver operating curves showed a similar trend (Fig. 7 B). The top 58 genes selected at least once in five of six models during cross-validation are depicted in Fig. 7 C. These include IFN-inducible and plasma cell-related transcripts, as well as transcripts related to platelet aggregation, angiogenesis, inflammation, and cell adhesion. Predicting OC using a similar machine learning approach yielded low accuracy, most likely due to the fact that OC includes a number of clinically heterogeneous complications and suggests that a larger sample size will be needed to develop independent classifiers for each of them. Overall, and although further validation in independent cohorts is warranted, our data suggest that early transcriptional changes in maternal blood might help predict PE in the context of SLE.

Discussion

SLE is characterized by failed tolerance to self, and maintenance of a successful pregnancy requires unique tolerance of paternally encoded antigens. It is therefore not surprising that SLE pregnancy carries a risk of complications. Early biomarkers to predict pregnancy outcome and help inform treatment to decrease morbidity and mortality are needed. This study aimed to assess maternal blood transcriptome dynamics during healthy pregnancy, from embryo implantation to postpartum, and to determine molecular changes associated with outcome in the context of SLE pregnancies.

We found that healthy pregnancy is characterized by a significant modulation of major transcriptional networks associated with SLE pathogenesis, including IFN, plasma cell, lymphoid, myeloid, and erythroid cell-related pathways (Banchereau et al.,

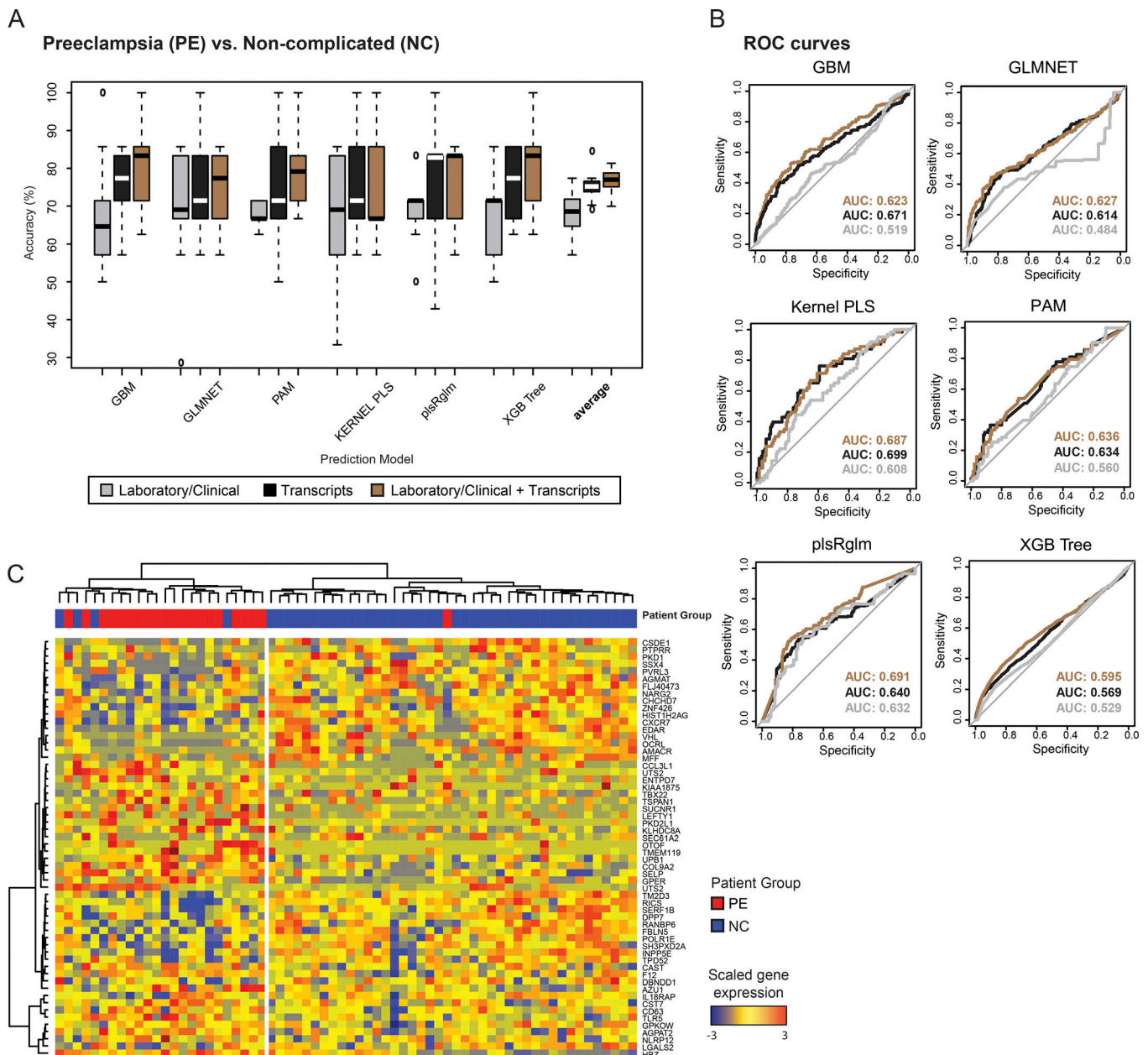


Figure 7. **Identification of a predictive transcriptional signature of SLE PE in the first trimester of pregnancy.** (A) Accuracy of different models predicting PE ($n = 21$) vs. NC ($n = 45$) at P1 using laboratory/clinical variables (gray) or gene expression only (black) or laboratory/clinical variables and gene expression combined (brown). (B) Receiver operator characteristic (ROC) curves of six models predicting PE vs. NC at P1 using laboratory/clinical variables only (gray), gene expression only (black), or both combined (brown). Area-under-the-curve (AUC) measures for each model are displayed in the bottom right corner. (C) Top 58 genes selected by 5 out of 6 models at least once during cross-validation from A. Scaled expression of the genes in PE and NC are shown. GBM, gradient boosting machine; GLMNET, generalized linear model via penalized maximum likelihood; kernel PLS, kernel partial least squares; PAM, prediction analysis for microarrays; plsRglm, partial least-squares regression for generalized linear models; XGB, eXtreme gradient boosting.

2016). Furthermore, these changes take place within days following embryo transfer, as detected in women undergoing ART. Importantly, immediately upon successful implantation an IFN-inducible transcriptionally spike is followed by down-regulation of the signature that persists through late pregnancy and PP. While this might be important to prevent the antiangiogenic milieu induced by IFN α (Andrade et al., 2015), down-regulation of the IFN response in human pregnancy could underlie the higher risk for certain infections such as influenza (Vanders et al., 2013),

as also described in an allogeneic mouse pregnancy model (Engels et al., 2017).

Persistent down-regulation of the IFN signature compared with the increased SLE nonpregnant baseline is mirrored in noncomplicated SLE pregnancy and supports the physiological relevance of this finding, especially since the IFN signature remained more prominent in complicated lupus pregnancies. It also supports recent reports that activation of the type I IFN/IFNAR axis in pregnancy primes for inflammation-driven

preterm birth in both mice and humans (Cappelletti et al., 2017; Engels et al., 2017). Whether the known association between SLE disease activity and pregnancy complications stems directly from increased IFN activity remains to be addressed (Molad et al., 2005; Clowse et al., 2008; Liu et al., 2012).

A recent study using mass cytometry revealed an increased STAT1 signaling response to ex vivo type I IFN in various innate and adaptive immune cells during pregnancy (Aghaepour et al., 2017). Our results suggest, in turn, that increased ex vivo IFN-inducible signaling might reflect a lower threshold for activation due to in vivo transcriptional repression of this response during pregnancy. Indeed, monocytes from both human and mouse neonates have been reported to respond to TLR4 stimulation with strong induction of TIR-domain-containing adapter-inducing interferon- β (TRIF)-dependent regulatory genes but weak activation of MyD88-dependent proinflammatory genes. This reciprocal shift was explained by the inverse baseline state of preactivated MyD88-dependent and barely detectable TRIF-dependent gene expression in neonatal versus adult monocytes (Ulas et al., 2017), which fits the transcriptional patterns we now describe in maternal blood during pregnancy.

In addition to the IFN signature, we detected sustained down-regulation of plasmablast/plasma cell signatures in both healthy and noncomplicated SLE pregnancies. These signatures, which are normally induced after infection and vaccination (Kardava et al., 2014; Kwissa et al., 2014; Athale et al., 2017), represent a robust biomarker of disease activity in pediatric SLE patients (Banchereau et al., 2016). Prolonged down-regulation of the plasma cell signature might be the result of either recruitment of antibody-secreting cells to the maternal–fetal interphase or active repression of terminal B cell differentiation programs. In fact, absolute counts of mature B cells are significantly lower, especially during the latest pregnancy stages (Kraus et al., 2012; Lima et al., 2016). This could be dependent on the inhibition of the IFN pathway, as type I IFN induces mature B cell survival and differentiation in multiple ways (Jego et al., 2003). Importantly, the plasma cell signature increased during the third trimester in SLE pregnancies associated with fetal complications. Thus, prospective studies to determine whether this signature represents an early biomarker of fetal complications are warranted.

Our study further reveals an up-regulation, in both healthy and noncomplicated SLE pregnancies, of innate immune signatures related to neutrophil, myeloid inflammation, and erythropoiesis pathways. Moreover, SLE pregnancy complicated by PE displayed the earliest (<15 wk) and most persistent up-regulation of the neutrophil signature, which correlated with an expansion of immature neutrophils. While glucocorticoid therapy has been linked to demargination of neutrophils, and this therapy was more frequently administered to SLE-PE patients at P1 compared with other groups (Table S6), daily glucocorticoid dose was low (prednisone <10 mg/d) and comparable between groups, and therefore unlikely to explain these changes (Guiducci et al., 2010).

The underlying mechanism and significance of neutrophil-related signatures in health and disease are not fully understood. These signatures might originate from more than one cell type,

including myeloid-derived suppressor cells, which characteristically express high levels of Arginase-1 and inducible nitric oxide synthase (Monu and Frey, 2012). An expansion of immature neutrophils with myeloid-derived suppressor cell features has been reported in healthy pregnancy (Blazkova et al., 2017). Immature neutrophils are also expanded in nonpregnant SLE patients (Bennett et al., 2003; Blazkova et al., 2017). Furthermore, NETs associate with higher rates of endothelial dysfunction and thrombosis (Elkon and Wiedeman, 2012). NETs are also highly enriched in infiltrating placental intervillous spaces in non-SLE pregnancy complicated with PE and in SLE pregnancy compared with healthy controls (Marder et al., 2016). An in-depth elucidation of the complexity of the neutrophil lineage expansion during pregnancy, and of its value as a predictive marker of SLE-associated PE, will require further studies.

Increased transcription of genes linked to the erythroid lineage has not been reported before in pregnancy but has been detected in subsets of children with bacterial infections (Ardura et al., 2009), autoinflammatory diseases (Allantaz et al., 2007; Fall et al., 2007), and active SLE (Banchereau et al., 2016). A subset of CD71⁺ erythroid cells, which are enriched in neonatal mice and human cord blood, displays unique immunosuppressive properties through expression of Arginase-2 (Elahi et al., 2013). More recently, two distinct populations of tumor-inducible, immunosuppressive erythroblast-like cells were described in the context of advanced tumors. These cells facilitate tumor progression by secreting the neurotrophic factor artemin into the blood or through the production of reactive oxygen species (Han et al., 2018; Zhao et al., 2018). Whether similar cells and/or mechanisms play a role during pregnancy also needs to be further addressed.

Supporting previous reports, we observed increased T and NK cell signatures in P3 and P4 associated with both OC and PE. Indeed, an expansion of ICOS⁺ total CD4⁺ and Tfh cells as well as transitional B cells was detected at earlier time points by FACS. Tfh cell dysregulation contributes to autoimmunity and allograft rejection (Nankivell and Alexander, 2010; Liu et al., 2013; Ueno et al., 2015). Similar cells accumulate within the uterus and placenta in a mouse model of allogeneic pregnancy and expand significantly upon PD-L1 blockade, which leads to fetal resorption (Zeng et al., 2016).

Our study identified early transcriptional changes performing better than previously reported laboratory/clinical parameters to predict PE. Among them, PKD1 and Oculocerebrorenal syndrome of Lowe protein are involved in apoptosis and renal tubulogenesis (Boletta et al., 2000; Bastos et al., 2009), TLR5 activation inhibits attachment of human trophoblast cells to endometrial cells (Aboussahoud et al., 2010), NLRP12 regulates human preimplantation development (Tuncer et al., 2014), and LEFTY1 inhibits decidualization (Li et al., 2014) and TGF β signaling (Ulloa and Tabibzadeh, 2001) and succinate receptor 1 (SUCNR1), which is linked to platelet activation (Macaulay et al., 2007) and to renovascular hypertension through activation of juxtaglomerular cells (Högberg et al., 2011; Mills and O'Neill, 2014). While this predictor list warrants validation, it uncovers potentially relevant mechanistic connections to SLE pregnancy complications. Recently, cell-free RNA transcripts in

maternal blood have been used for predicting gestational age and preterm delivery (Ngo et al., 2018). These transcripts did not overlap with our cell-associated predictive transcripts, but the synergy of these noninvasive approaches should be explored in future prospective studies.

Our study identifies significant modulation of transcriptional and cellular immune pathways during healthy pregnancy that may facilitate implantation of the semi-allogeneic fetus. These pathways are also linked to SLE pathogenesis, and failure to modulate them is associated with lupus pregnancy complications. Our findings provide a framework for future studies aimed at investigating these immunological pathways and developing therapeutic strategies to improve health outcomes for mothers with SLE and their offspring.

Materials and methods

Study design

PROMISSE cohort

PROMISSE is a multicenter, prospective observational study of pregnancies in women with SLE (four or more revised American College of Rheumatology criteria; Hochberg, 1997) and/or anti-phospholipid antibodies (Miyakis et al., 2006), as well as healthy controls at low risk of adverse outcomes (one or more successful pregnancy; no prior fetal death; and fewer than two miscarriages at <10 WG; Buyon et al., 2015). All patients were recruited at <12 WG. This study focuses on patients enrolled between September 2003 and August 2013 from six sites in the United States and one in Canada. All mechanistic studies, including microarray and flow cytometry, were performed at the Baylor Institute for Immunology Research. The following institutional review committees from the recruiting organizations approved sample collection, sample receipt, and research performed as part of this study: Hospital for Special Surgery Institutional Review Board (IRB), Intermountain Health Care Urban Central Region IRB (Utah), NYU School of Medicine IRB, Oklahoma Medical Research Foundation IRB, The Johns Hopkins Medical Institutions (Western IRB), The University of Chicago IRB, Mt. Sinai Hospital's Research Ethics Committee (Toronto, Canada), and University of Utah IRB. Patients with SLE had inactive or mild/moderate activity at screening (mean SLEPDAI score = 3.01). Exclusion criteria were prednisone >20 mg/d, urinary protein/creatinine ratio >1,000 mg/g, erythrocyte casts, serum creatinine level >1.2 mg/deciliter, diabetes mellitus, and blood pressure >140/90 mm Hg at screening. Detailed medical and obstetrical information and serial blood samples were collected each month during the course of pregnancy. IRBs approved the protocol, and written, informed consent was obtained from all participants.

Adverse pregnancy outcomes were defined as one or more of the following: (1) PE at any time (ACOG Committee on Practice Bulletins—Obstetrics, 2002); (2) fetal death at >12 WG unexplained by chromosomal abnormality, anatomical malformation, or congenital infection; (3) neonatal death before hospital discharge due to complications of prematurity; (4) preterm delivery or termination of pregnancy at <36 WG due to growth restriction or placental insufficiency; and (5) small for gestational age of

less than the fifth percentile at birth. We subdivided patients into those with PE and those with OC.

Our target sample size was 40 SLE pregnancies without complications, 40 SLE pregnancies with complications (20 with PE; 20 with OC), and 40 healthy control subjects who had complete sets of PreAnalytiX blood RNA (PAXgene) tubes (Qiagen) for each time point of interest. However, to avoid dropouts due to sample processing, a few extra patients were included in each group. We identified 46 SLE patients with complications who had complete sets of PAX gene tubes available for analysis and collected at the following intervals: <16 WG, 16–23 WG, 24–31 WG, 32–40 WG (if still pregnant), and 8–20 wk PP (Fig. 1 B). For comparison groups, we selected the first 46 SLE-NC and 43 H-P. We also enrolled 23 H-NP controls. Laboratory values and demographics of SLE patients are summarized in Table S6.

For SLE-NP and additional H-NP, 82 subjects (62 SLE-NP and 20 H-NP individuals) were obtained from NCBI GEO (accession no. GSE49454). These samples were originally hybridized on the same platform (Illumina HT-12 V4 beadchips) and in the same facility. Exclusion criteria included (1) current treatment with mycophenolate mofetil or cyclophosphamide, (2) active renal flare, (3) patient >43 yr, and (4) male patient. When patients had multiple visits, the sample with the lowest SLEPDAI score was chosen, resulting in the selection of 20 unique SLE-NP and 11 H-NP samples. There were no demographic, clinical, or disease activity differences between pregnant and nonpregnant patient groups (Table S6).

ART cohort

An independent cohort of healthy women undergoing ART was recruited at the University of Connecticut Center for Advanced Reproductive Services from November 2014 to July 2015. The protocol was approved by the Independent Review Board of the University of Connecticut Health Center (IRB no.15-057J-3). Subjects who were <37 yr of age with normal ovarian reserve and undergoing blastocyst transfer were included in the study. Women with recent vaccination (within 14 d), chronic infection, or autoimmune disorders were excluded. Whole blood was collected in Tempus tubes on the day of embryo transfer, midluteal, and on the day of scheduled pregnancy test. Those who conceived (defined as positive pregnancy test) were asked to submit an additional sample between 6 and 8 WG (PO). Of the 40 subjects enrolled, 25 were included in the final analysis. The clinical protocol from seven subjects was terminated before embryo transfer, and samples from eight subjects failed quality control.

Whole-blood flow cytometry staining

Whole-blood samples were collected throughout pregnancy from 50 individuals from PROMISSE for flow cytometry. This convenience sample, based on practical conditions of patient availability, yielded 125 blood samples: P1–4 and PP for H-P ($n = 11$) and SLE-NC ($n = 30$) and, due to scarcity and early delivery in complicated group, P1–2 for SLE-PE ($n = 5$) and SLE-OC ($n = 4$) samples were collected. Acid citrate dextrose–anticoagulated whole blood was aliquoted at 200 μ l/tube to six 5-ml Falcon tubes (BD Biosciences) for control staining and phenotyping of

B cells, monocytes and granulocytes, Tfh cells, dendritic cells, T regulatory cells, and NK cells. Blood was incubated with monoclonal antibodies for 15 min at room temperature, followed by RBC lysis with BD FACSLyse Buffer (BD Biosciences) for 10 min at room temperature in the dark, and two washing steps with PBS. Samples were acquired on a custom BD LSR Fortessa. The gating strategy used herein was previously described (Maecker et al., 2012; Obermoser et al., 2013). Data were analyzed in Flowjo 9.8 software. FACS antibodies are listed in Table S8.

RNA extraction and microarray processing for the PROMISSE cohort

Total RNA was extracted as previously described (Berry et al., 2010). Amplified RNA was hybridized to Illumina HT-12 V4 beadchips (47,231 probes) and scanned on an Illumina Beadstation 500. Signal-intensity values were generated using Illumina's GenomeStudio version 2011.1 with the Gene Expression Module v1.9.0 (Illumina). Background subtraction and average normalization were performed using GenomeStudio. The microarray dataset described in this manuscript is deposited in the NCBI GEO (accession no. GSE108497).

RNA sequencing for ART cohort

RNA was isolated and globin-reduced using the Tempus Spin RNA kit (Applied Biosystems/Ambion) and the GLOBINclear kit (Applied Biosystems/Ambion), respectively. Illumina barcoded stranded RNA-seq libraries were prepared and sequenced using either the Illumina HiSeq2500 or NextSeq500 targeting 30 million paired-end reads (2×75 bp) per sample. FASTQ files were created using the Illumina CASAVA v1.8.2 pipeline. The sequencing reads generated by the pipeline were further subjected to quality control using NGSQC toolkit v2.3 and samples with at least 70% of the nucleotides having base quality >30 were included in the analysis. High-quality reads were mapped to human transcriptome from ENSEMBL build 70 based on the NCBI human genome version 37. Alignments were made with TopHat v2.0 and then subsequent transcript and gene-level counts, fragments per kilobase of transcript per million reads, and transcripts per million values were obtained using RSEM using the default parameters. The RNA-seq data for ART is deposited in BioProject (accession no. PRJNA427177).

Linear mixed models

Two linear mixed models were developed to identify DETs in microarray (A) or differentially expressed flow subsets (B). To exploit longitudinal and repeated measures, all models consisted of a patient-specific random intercept and specific fixed effects. Spatial power covariance structures were used for all linear mixed models to explain regular intervals between repeated measurements. Estimate statements were used to test for comparisons of interest. Models used the SAS MIXED procedure using *sp(pow)* type and were run in JMP Genomics 6.0 (SAS Institute, Inc.). Detailed SAS codes are provided in Table S10.

(A) SAS Linear Mixed model code for microarray

The first model was designed to identify DETs correlated with disease, pregnancy, complication group, and time point. APO = Adverse Pregnancy Outcome (PE + OC).

(B) SAS Linear Mixed model code for flow cytometry analysis

The second linear mixed model was developed to identify FACS subsets correlated with complication group and time point.

Batch normalization

Our dataset was normalized with batch correction method using JMP Genomics 6.0 after standardizing for batch (SAS Institute, Inc.). Briefly, datasets from two batches were normalized by establishing a batch profile based on averaging across within-batch-level H-NP controls and then applying this profile to correct values across batches to all the other samples. K-mean clustering is used for grouping batch profiles into clusters.

Modular transcriptional analysis

A preexisting framework of 260 coexpressed transcriptional modules was used (Chaussabel and Baldwin, 2014). For simplicity, only the 97 modules forming the first seven rounds of selection of the module set were represented. For each module, the percentage of probes significantly up- or down-regulated in the pregnant group was calculated based on the linear mixed-model result. The module score was calculated based on the percentage of genes within a module that are significantly (FDR < 0.05) upregulated minus the percentage of genes within a module that are significantly down-regulated (within a given comparison). Gene lists for Baylor whole blood modules are listed in Table S9.

Q-Gen analysis

Q-Gen is a generalization of the QuSAGE algorithm (Yaari et al., 2013) that integrates statistics from mixed-model analysis by conducting necessary estimation adjustments (Turner et al., 2015). Modules with at least 15 transcripts were considered for QuSAGE analysis. Significantly enriched gene sets (blood modules) were selected based on two criteria: (1) FDR < 0.05 and (2) FC ≥ 1.3 or ≤ 0.7 in the comparison considered in the training set.

Predictive modeling

Predictive modeling was performed using the Caret package. ROC curves are generated using the pROC.

GenBart interface

GenBart files are generated using genBART R package. BART (Biostatistical Analysis Reporting Tool) is a user-friendly, point-and-click, R shiny application. The analysis results were formatted and combined to an R datafile to be uploaded and efficiently examined (available at <https://data.mendeley.com/datasets/hg596dwd6/1>; Hong, 2018). BART provides users the ability to easily view, modify, and download the tables and figures generated by the app.

Online supplemental material

Fig. S1 shows line graphs of significantly differentiated modules in SLE-complicated groups in Fig. 6 B normalized to H-NP. Fig. S2 compares blood module signatures of SLE-PE and SLE-OC with or without adjustment by SLEPDAI score at initial visit. Fig. S3 represents a summary of the main features of genBart shiny app. Table S1 shows demographics, embryo transfer method, and

estradiol level before embryo transfer categorized by pregnancy status for the ART cohort. Table S2 shows Q-Gen results based on a mixed-model analysis using blood modules as gene sets. Table S3 shows absolute counts of 84 blood cell subsets measured by flow cytometry. Table S4 shows flow cytometry populations ($n = 43$) significantly changed in a linear mixed model ($P \leq 0.05$). Table S5 shows Q-Gen results based on a linear mixed model using blood modules as gene sets for the ART cohort. Table S6 shows demographics, laboratory values, SLE activity, and medications of SLE patients from the PROMISSE cohort during pregnancy. Table S7 lists predictors' variable importance and their significant index of 8,201 genes in five PE prediction models. Table S8 shows an antibodies list used for flow cytometry. Table S9 shows gene lists corresponding to whole-blood modules. Table S10 shows detailed SAS codes.

Acknowledgments

We are grateful to the SLE patients and healthy subjects who participated in our study and M.D. Lockshin for help with recruiting patients.

This work was supported by the National Institute of Arthritis and Musculoskeletal and Skin Diseases/National Institutes of Health awards R01 AR49772 and R01 AR49772-07S2 (J.E. Salmon), R01 AR69572 and AR43727 (M. Petri), National Institute of Allergy and Infectious Diseases/National Institutes of Health award U19 AI082715 (V. Pascual), P50AR070594 (V. Pascual and J. Banchereau), the Morris and Alma Schapiro Fund (J.E. Salmon), the Baylor-Scott & White Health Care Research Foundation, and the Kathryn W. Davis gift to the Jackson Laboratory.

Author contributions: S. Hong and R. Banchereau analyzed data and wrote the manuscript. B-S.L. Maslow, J. Nulsen, and J. Banchereau recruited and generated the ART data. S. Hong, B-S.L. Maslow, and D. Nehar-Belaid analyzed the ART data. M. M. Guerra collected clinical data and revised the manuscript. J. Baisch, D.W. Branch, T.F. Porter, A. Sawitzke, C.A. Laskin, J.P. Buyon, J.T. Merrill, L.R. Sammaritano, and M. Petri followed PROMISSE patients and collected clinical data and samples. S. Hong, J. Turner, J. Cardenas, and D. Blankenship conducted statistical analysis, developed models, and developed the GenBart interface. E. Gatewood, A-M. Cepika, M. Ohouo, T.W. Kim, and G. Obermoser generated and interpreted FACS analysis. E. Anguiano supervised microarray. V. Pascual, J.E. Salmon, and J. Banchereau supervised the study, interpreted data, and wrote the manuscript.

The authors declare no competing financial interests.

Submitted: 29 January 2019

Revised: 28 February 2019

Accepted: 4 March 2019

References

Aboussahoud, W., C. Bruce, S. Elliott, and A. Fazeli. 2010. Activation of Toll-like receptor 5 decreases the attachment of human trophoblast cells to endometrial cells in vitro. *Hum. Reprod.* 25:2217–2228. <https://doi.org/10.1093/humrep/deq185>

ACOG Committee on Practice Bulletins–Obstetrics. 2002. ACOG practice bulletin. Diagnosis and management of preeclampsia and eclampsia. Number 33, January 2002. *Obstet. Gynecol.* 99:159–167.

Aghaepour, N., E.A. Ganio, D. McIlwain, A.S. Tsai, M. Tingle, S. Van Gassen, D.K. Gaudilliere, Q. Baca, L. McNeil, R. Okada, et al. 2017. An immune clock of human pregnancy. *Sci. Immunol.* 2:eaan2946. <https://doi.org/10.1126/sciimmunol.aan2946>

Allantaz, F., D. Chaussabel, D. Stichweh, L. Bennett, W. Allman, A. Mejias, M. Ardura, W. Chung, E. Smith, C. Wise, et al. 2007. Blood leukocyte microarrays to diagnose systemic onset juvenile idiopathic arthritis and follow the response to IL-1 blockade [published correction appears in *J Exp. Med.* 2009;206(10):2299]. *J. Exp. Med.* 204:2131–2144. <https://doi.org/10.1084/jem.20070070>

Andrade, D., M. Kim, L.P. Blanco, S.A. Karumanchi, G.C. Koo, P. Redecha, K. Kirou, A.M. Alvarez, M.J. Mulla, M.K. Crow, et al. 2015. Interferon- α and angiogenic dysregulation in pregnant lupus patients who develop preeclampsia. *Arthritis Rheumatol.* 67:977–987. <https://doi.org/10.1002/art.39029>

Ardura, M.I., R. Banchereau, A. Mejias, T. Di Pucchio, C. Glaser, F. Allantaz, V. Pascual, J. Banchereau, D. Chaussabel, and O. Ramilo. 2009. Enhanced monocyte response and decreased central memory T cells in children with invasive *Staphylococcus aureus* infections. *PLoS One.* 4:e5446. <https://doi.org/10.1371/journal.pone.0005446>

Athale, S., R. Banchereau, L. Thompson-Snipes, Y. Wang, K. Palucka, V. Pascual, and J. Banchereau. 2017. Influenza vaccines differentially regulate the interferon response in human dendritic cell subsets. *Sci. Transl. Med.* 9:eaaf9194. <https://doi.org/10.1126/scitranslmed.aaf9194>

Baechler, E.C., F.M. Batliwalla, G. Karypis, P.M. Gaffney, W.A. Ortmann, K.J. Espe, K.B. Shark, W.J. Grande, K.M. Hughes, V. Kapur, et al. 2003. Interferon-inducible gene expression signature in peripheral blood cells of patients with severe lupus. *Proc. Natl. Acad. Sci. USA.* 100:2610–2615. <https://doi.org/10.1073/pnas.0337691100>

Banchereau, R., S. Hong, B. Cantarel, N. Baldwin, J. Baisch, M. Edens, A.M. Cepika, P. Acs, J. Turner, E. Anguiano, et al. 2016. Personalized immunomonitoring uncovers molecular networks that stratify lupus patients. *Cell.* 165:551–565. <https://doi.org/10.1016/j.cell.2016.03.008>

Bastos, A.P., K. Piontek, A.M. Silva, D. Martini, L.F. Menezes, J.M. Fonseca, I.I. Fonseca, G.G. Germino, and L.F. Onuchic. 2009. Pkd1 haploinsufficiency increases renal damage and induces microcyst formation following ischemia/reperfusion. *J. Am. Soc. Nephrol.* 20:2389–2402. <https://doi.org/10.1681/ASN.2008040435>

Bennett, L., A.K. Palucka, E. Arce, V. Cantrell, J. Borvak, J. Banchereau, and V. Pascual. 2003. Interferon and granulopoiesis signatures in systemic lupus erythematosus blood. *J. Exp. Med.* 197:711–723. <https://doi.org/10.1084/jem.20021553>

Berman, J., G. Girardi, and J.E. Salmon. 2005. TNF- α is a critical effector and a target for therapy in antiphospholipid antibody-induced pregnancy loss. *J. Immunol.* 174:485–490. <https://doi.org/10.4049/jimmunol.174.1.485>

Berry, M.P., C.M. Graham, F.W. McNab, Z. Xu, S.A. Bloch, T. Oni, K.A. Wilkinson, R. Banchereau, J. Skinner, R.J. Wilkinson, et al. 2010. An interferon-inducible neutrophil-driven blood transcriptional signature in human tuberculosis. *Nature.* 466:973–977. <https://doi.org/10.1038/nature09247>

Blazkova, J., S. Gupta, Y. Liu, B. Gaudilliere, E.A. Ganio, C.R. Bolen, R. Saardover, G.K. Fragiadakis, M.S. Angst, S. Hasni, et al. 2017. Multicenter systems analysis of human blood reveals immature neutrophils in males and during pregnancy. *J. Immunol.* 198:2479–2488. <https://doi.org/10.4049/jimmunol.1601855>

Boletta, A., F. Qian, L.F. Onuchic, A.K. Bhunia, B. Phakdeekitcharoen, K. Hanaoka, W. Guggino, L. Monaco, and G.G. Germino. 2000. Polycystin-1, the gene product of PKD1, induces resistance to apoptosis and spontaneous tubulogenesis in MDCK cells. *Mol. Cell.* 6:1267–1273. [https://doi.org/10.1016/S1097-2765\(00\)00123-4](https://doi.org/10.1016/S1097-2765(00)00123-4)

Bundhun, P.K., M.Z. Soogund, and F. Huang. 2017. Impact of systemic lupus erythematosus on maternal and fetal outcomes following pregnancy: A meta-analysis of studies published between years 2001–2016. *J. Autoimmun.* 79:17–27. <https://doi.org/10.1016/j.jaut.2017.02.009>

Buyon, J.P., M.Y. Kim, M.M. Guerra, C.A. Laskin, M. Petri, M.D. Lockshin, L. Sammaritano, D.W. Branch, T.F. Porter, A. Sawitzke, et al. 2015. Predictors of pregnancy outcomes in patients with lupus: a cohort study. *Ann. Intern. Med.* 163:153–163. <https://doi.org/10.7326/M14-2235>

Caielli, S., S. Athale, B. Domic, E. Murat, M. Chandra, R. Banchereau, J. Baisch, K. Phelps, S. Clayton, M. Gong, et al. 2016. Oxidized mitochondrial nucleoids released by neutrophils drive type I interferon production in human lupus. *J. Exp. Med.* 213:697–713. <https://doi.org/10.1084/jem.20151876>

Cappelletti, M., P. Presicce, M.J. Lawson, V. Chaturvedi, T.E. Stankiewicz, S. Vanoni, I.T. Harley, J.W. McAlees, D.A. Giles, M.E. Moreno-Fernandez,

- et al. 2017. Type I interferons regulate susceptibility to inflammation-induced preterm birth. *JCI Insight*. 2:e91288. <https://doi.org/10.1172/jci.insight.91288>
- Chaussabel, D., and N. Baldwin. 2014. Democratizing systems immunology with modular transcriptional repertoire analyses. *Nat. Rev. Immunol.* 14: 271–280. <https://doi.org/10.1038/nri3642>
- Chaussabel, D., C. Quinn, J. Shen, P. Patel, C. Glaser, N. Baldwin, D. Stichweh, D. Blankenship, L. Li, I. Munagala, et al. 2008. A modular analysis framework for blood genomics studies: application to systemic lupus erythematosus. *Immunity*. 29:150–164. <https://doi.org/10.1016/j.immuni.2008.05.012>
- Chiche, L., N. Jourde-Chiche, E. Whalen, S. Presnell, V. Gersuk, K. Dang, E. Anguiano, C. Quinn, S. Burtey, Y. Berland, et al. 2014. Modular transcriptional repertoire analyses of adults with systemic lupus erythematosus reveal distinct type I and type II interferon signatures. *Arthritis Rheumatol.* 66:1583–1595. <https://doi.org/10.1002/art.38628>
- Clowse, M.E., L.S. Magder, F. Witter, and M. Petri. 2005. The impact of increased lupus activity on obstetric outcomes. *Arthritis Rheum.* 52: 514–521. <https://doi.org/10.1002/art.20864>
- Clowse, M.E., M. Jamison, E. Myers, and A.H. James. 2008. A national study of the complications of lupus in pregnancy. *Am. J. Obstet. Gynecol.* 199:e121–e126.
- Cohen, D., A. Buurma, N.N. Goemaere, G. Girardi, S. le Cessie, S. Scherjon, K. W. Bloemenkamp, E. de Heer, J.A. Bruijn, and I.M. Bajema. 2011. Classical complement activation as a footprint for murine and human antiphospholipid antibody-induced fetal loss. *J. Pathol.* 225:502–511. <https://doi.org/10.1002/path.2893>
- Elahi, S., J.M. Ertelt, J.M. Kinder, T.T. Jiang, X. Zhang, L. Xin, V. Chaturvedi, B. S. Strong, J.E. Qualls, K.A. Steinbrecher, et al. 2013. Immunosuppressive CD71+ erythroid cells compromise neonatal host defence against infection. *Nature*. 504:158–162. <https://doi.org/10.1038/nature12675>
- Elkon, K.B., and A. Wiedeman. 2012. Type I IFN system in the development and manifestations of SLE. *Curr. Opin. Rheumatol.* 24:499–505. <https://doi.org/10.1097/BOR.0b013e3283526c3e>
- Engels, G., A.M. Hierweiger, J. Hoffmann, R. Thieme, S. Thiele, S. Bertram, C. Dreier, P. Resa-Infante, H. Jacobsen, K. Thiele, et al. 2017. Pregnancy-related immune adaptation promotes the emergence of highly virulent H1N1 influenza virus strains in allogeneically pregnant mice. *Cell Host Microbe*. 21:321–333. <https://doi.org/10.1016/j.chom.2017.02.020>
- Fall, N., M. Barnes, S. Thornton, L. Luyrink, J. Olson, N.T. Ilowite, B.S. Gottlieb, T. Griffin, D.D. Sherry, S. Thompson, et al. 2007. Gene expression profiling of peripheral blood from patients with untreated new-onset systemic juvenile idiopathic arthritis reveals molecular heterogeneity that may predict macrophage activation syndrome. *Arthritis Rheum.* 56: 3793–3804. <https://doi.org/10.1002/art.22981>
- Gack, S., A. Marmé, F. Marmé, G. Wrobel, B. Vonderstrass, G. Bastert, P. Lichter, P. Angel, and M. Schorpp-Kistner. 2005. Preeclampsia: increased expression of soluble ADAM 12. *J. Mol. Med. (Berl.)*. 83:887–896. <https://doi.org/10.1007/s00109-005-0714-9>
- Gelber, S.E., E. Brent, P. Redecha, G. Perino, S. Tomlinson, R.L. Davison, and J.E. Salmon. 2015. Prevention of defective placentation and pregnancy loss by blocking innate immune pathways in a syngeneic model of placental insufficiency. *J. Immunol.* 195:1129–1138. <https://doi.org/10.4049/jimmunol.1402220>
- Girardi, G., J. Bertram, P. Redecha, L. Spruce, J.M. Thurman, D. Kraus, T.J. Hollmann, P. Casali, M.C. Carroll, R.A. Wetsel, et al. 2003. Complement C5a receptors and neutrophils mediate fetal injury in the antiphospholipid syndrome. *J. Clin. Invest.* 112:1644–1654. <https://doi.org/10.1172/JCI200318817>
- Girardi, G., D. Yarilin, J.M. Thurman, V.M. Holers, and J.E. Salmon. 2006. Complement activation induces dysregulation of angiogenic factors and causes fetal rejection and growth restriction. *J. Exp. Med.* 203:2165–2175. <https://doi.org/10.1084/jem.20061022>
- Guiducci, C., M. Gong, Z. Xu, M. Gill, D. Chaussabel, T. Meeker, J.H. Chan, T. Wright, M. Punaro, S. Bolland, et al. 2010. TLR recognition of self nucleic acids hampers glucocorticoid activity in lupus. *Nature*. 465: 937–941. <https://doi.org/10.1038/nature09102>
- Han, Y., Q. Liu, J. Hou, Y. Gu, Y. Zhang, Z. Chen, J. Fan, W. Zhou, S. Qiu, Y. Zhang, et al. 2018. Tumor-induced generation of splenic erythroblast-like Ter-cells promotes tumor progression. *Cell*. 173:634–648.
- Hochberg, M.C. 1997. Updating the American College of Rheumatology revised criteria for the classification of systemic lupus erythematosus. *Arthritis Rheum.* 40:1725 (Letter) (PMID: 9324032). <https://doi.org/10.1002/art.1780400928>
- Högberg, C., O. Gidlöf, C. Tan, S. Svensson, J. Nilsson-Öhman, D. Erlinge, and B. Olde. 2011. Succinate independently stimulates full platelet activation via cAMP and phosphoinositide 3-kinase- β signaling. *J. Thromb. Haemost.* 9:361–372. <https://doi.org/10.1111/j.1538-7836.2010.04158.x>
- Hong, Seunghee. 2018. genBart file for PROMISSE manuscript. Mendeley Data, v1. Available at: <http://dx.doi.org/10.17632/hg596dwdwr.1> (accessed March 27, 2019).
- Hunt, J.S., and D.E. Geraghty. 2005. Soluble HLA-G isoforms: technical deficiencies lead to misinterpretations. *Mol. Hum. Reprod.* 11:715–717. <https://doi.org/10.1093/molehr/gah223>
- Jego, G., A.K. Palucka, J.P. Blanck, C. Chalouni, V. Pascual, and J. Banchereau. 2003. Plasmacytoid dendritic cells induce plasma cell differentiation through type I interferon and interleukin 6. *Immunity*. 19:225–234. [https://doi.org/10.1016/S1074-7613\(03\)00208-5](https://doi.org/10.1016/S1074-7613(03)00208-5)
- Jiang, T.T., V. Chaturvedi, J.M. Ertelt, J.M. Kinder, D.R. Clark, A.M. Valent, L. Xin, and S.S. Way. 2014. Regulatory T cells: new keys for further unlocking the enigma of fetal tolerance and pregnancy complications. *J. Immunol.* 192:4949–4956. <https://doi.org/10.4049/jimmunol.1400498>
- Kardava, L., S. Moir, N. Shah, W. Wang, R. Wilson, C.M. Buckner, B.H. Santich, L.J. Kim, E.E. Spurlin, A.K. Nelson, et al. 2014. Abnormal B cell memory subsets dominate HIV-specific responses in infected individuals. *J. Clin. Invest.* 124:3252–3262. <https://doi.org/10.1172/JCI74351>
- Kim, M.Y., J.P. Buyon, M.M. Guerra, S. Rana, D. Zhang, C.A. Laskin, M. Petri, M.D. Lockshin, L.R. Sammaritano, D.W. Branch, T.F. et al. 2016. Angiogenic factor imbalance early in pregnancy predicts adverse outcomes in patients with lupus and antiphospholipid antibodies: results of the PROMISSE study. *Am. J. Obstet. Gynecol.* 214:e101–e108e114.
- Kitaya, K., T. Yasuo, T. Yamaguchi, S. Fushiki, and H. Honjo. 2007. Genes regulated by interferon-gamma in human uterine microvascular endothelial cells. *Int. J. Mol. Med.* 20:689–697.
- Kraus, T.A., S.M. Engel, R.S. Sperling, L. Kellerman, Y. Lo, S. Wallenstein, M. M. Escribese, J.L. Garrido, T. Singh, M. Loubeau, et al. 2012. Characterizing the pregnancy immune phenotype: results of the viral immunity and pregnancy (VIP) study. *J. Clin. Immunol.* 32:300–311. <https://doi.org/10.1007/s10875-011-9627-2>
- Kwissa, M., H.I. Nakaya, N. Onlamoon, J. Wrammert, F. Villinger, G.C. Perng, S. Yoksan, K. Pattanapanyasat, K. Chokephaibulkit, R. Ahmed, et al. 2014. Dengue virus infection induces expansion of a CD14(+)CD16(+) monocyte population that stimulates plasmablast differentiation. *Cell Host Microbe*. 16:115–127. <https://doi.org/10.1016/j.chom.2014.06.001>
- Li, H., H. Li, L. Bai, and H. Yu. 2014. Lefty inhibits in vitro decidualization by regulating P57 and cyclin D1 expressions. *Cell Biochem. Funct.* 32: 657–664. <https://doi.org/10.1002/cbf.3069>
- Lima, J., C. Martins, M.J. Leandro, G. Nunes, M.J. Sousa, J.C. Branco, and L.M. Borrego. 2016. Characterization of B cells in healthy pregnant women from late pregnancy to post-partum: a prospective observational study. *BMC Pregnancy Childbirth*. 16:139. <https://doi.org/10.1186/s12884-016-0927-7>
- Liu, J., Y. Zhao, Y. Song, W. Zhang, X. Bian, J. Yang, D. Liu, X. Zeng, and F. Zhang. 2012. Pregnancy in women with systemic lupus erythematosus: a retrospective study of 111 pregnancies in Chinese women. *J. Matern. Fetal Neonatal Med.* 25:261–266.
- Liu, Z., H. Fan, and S. Jiang. 2013. CD4(+) T-cell subsets in transplantation. *Immunol. Rev.* 252:183–191. <https://doi.org/10.1111/imr.12038>
- Lood, C., L.P. Blanco, M.M. Purmalek, C. Carmona-Rivera, S.S. De Ravin, C.K. Smith, H.L. Maleck, J.A. Ledbetter, K.B. Elkon, and M.J. Kaplan. 2016. Neutrophil extracellular traps enriched in oxidized mitochondrial DNA are interferogenic and contribute to lupus-like disease. *Nat. Med.* 22: 146–153. <https://doi.org/10.1038/nm.4027>
- Macaulay, I.C., M.R. Tijssen, D.C. Thijssen-Timmer, A. Gusnanto, M. Steward, P. Burns, C.F. Langford, P.D. Ellis, F. Dudbridge, J.J. Zwaginga, et al. 2007. Comparative gene expression profiling of in vitro differentiated megakaryocytes and erythroblasts identifies novel activatory and inhibitory platelet membrane proteins. *Blood*. 109:3260–3269. <https://doi.org/10.1182/blood-2006-07-036269>
- Maecker, H.T., J.P. McCoy, and R. Nussenblatt. 2012. Standardizing immunophenotyping for the Human Immunology Project. *Nat. Rev. Immunol.* 12:191–200. <https://doi.org/10.1038/nri3158>
- Marder, W., J.S. Knight, M.J. Kaplan, E.C. Somers, X. Zhang, A.A. O'Dell, V. Padmanabhan, and R.W. Lieberman. 2016. Placental histology and neutrophil extracellular traps in lupus and pre-eclampsia pregnancies. *Lupus Sci. Med.* 3:e000134. <https://doi.org/10.1136/lupus-2015-000134>
- Mills, E., and L.A. O'Neill. 2014. Succinate: a metabolic signal in inflammation. *Trends Cell Biol.* 24:313–320. <https://doi.org/10.1016/j.tcb.2013.11.008>
- Miyakis, S., M.D. Lockshin, T. Atsumi, D.W. Branch, R.L. Brey, R. Cervera, R. H. Derksen, P.G. De Groot, T. Koike, P.L. Meroni, et al. 2006.

- International consensus statement on an update of the classification criteria for definite antiphospholipid syndrome (APS). *J. Thromb. Haemost.* 4:295–306. <https://doi.org/10.1111/j.1538-7836.2006.01753.x>
- Molad, Y., T. Borkowski, A. Monselise, A. Ben-Haroush, J. Sulkes, M. Hod, D. Feldberg, and J. Bar. 2005. Maternal and fetal outcome of lupus pregnancy: a prospective study of 29 pregnancies. *Lupus*. 14:145–151. <https://doi.org/10.1191/0961203305lu2072oa>
- Monu, N.R., and A.B. Frey. 2012. Myeloid-derived suppressor cells and anti-tumor T cells: a complex relationship. *Immunol. Invest.* 41:595–613. <https://doi.org/10.3109/08820139.2012.673191>
- Mor, G., P. Aldo, and A.B. Alvero. 2017. The unique immunological and microbial aspects of pregnancy. *Nat. Rev. Immunol.* 17:469–482. <https://doi.org/10.1038/nri.2017.64>
- Nankivell, B.J., and S.I. Alexander. 2010. Rejection of the kidney allograft. *N. Engl. J. Med.* 363:1451–1462. <https://doi.org/10.1056/NEJMra0902927>
- Ngo, T.T.M., M.N. Moufarrej, M.H. Rasmussen, J. Camunas-Soler, W. Pan, J. Okamoto, N.F. Neff, K. Liu, R.J. Wong, K. Downes, et al. 2018. Noninvasive blood tests for fetal development predict gestational age and preterm delivery. *Science*. 360:1133–1136. <https://doi.org/10.1126/science.aar3819>
- Obermoser, G., S. Presnell, K. Domico, H. Xu, Y. Wang, E. Anguiano, L. Thompson-Snipes, R. Ranganathan, B. Zeitner, A. Bjork, et al. 2013. Systems scale interactive exploration reveals quantitative and qualitative differences in response to influenza and pneumococcal vaccines. *Immunity*. 38:831–844. <https://doi.org/10.1016/j.immuni.2012.12.008>
- PrabhuDas, M., E. Bonney, K. Caron, S. Dey, A. Erlebacher, A. Fazleabas, S. Fisher, T. Golos, M. Matzuk, J.M. McCune, et al. 2015. Immune mechanisms at the maternal-fetal interface: perspectives and challenges. *Nat. Immunol.* 16:328–334. <https://doi.org/10.1038/ni.3131>
- Rusinova, I., S. Forster, S. Yu, A. Kannan, M. Masse, H. Cumming, R. Chapman, and P.J. Hertzog. 2013. Interferome v2.0: an updated database of annotated interferon-regulated genes. *Nucleic Acids Res.* 41(D1): D1040–D1046. <https://doi.org/10.1093/nar/gks1215>
- Schmidt, A., P. Groth, B. Haendler, H. Hess-Stumpp, J. Krätzschmar, H. Seidel, M. Thaele, and B. Weiss. 2005. Gene expression during the implantation window: microarray analysis of human endometrial samples. *Ernst Schering Res. Found. Workshop*. 52:139–157. https://doi.org/10.1007/3-540-27147-3_7
- Shamonki, J.M., J.E. Salmon, E. Hyjek, and R.N. Baergen. 2007. Excessive complement activation is associated with placental injury in patients with antiphospholipid antibodies. *Am. J. Obstet. Gynecol.* 196:e161–e165.
- Textoris, J., D. Ivorra, A. Ben Amara, F. Sabatier, J.P. Ménard, H. Heckenroth, F. Bretelle, and J.L. Mege. 2013. Evaluation of current and new biomarkers in severe preeclampsia: a microarray approach reveals the VSIG4 gene as a potential blood biomarker. *PLoS One*. 8:e82638. <https://doi.org/10.1371/journal.pone.0082638>
- Tuncer, S., M.T. Fiorillo, and R. Sorrentino. 2014. The multifaceted nature of NLRP12. *J. Leukoc. Biol.* 96:991–1000. <https://doi.org/10.1189/jlb.3RU0514-265RR>
- Turner, J.A., C.R. Bolen, and D.M. Blankenship. 2015. Quantitative gene set analysis generalized for repeated measures, confounder adjustment, and continuous covariates. *BMC Bioinformatics*. 16:272. <https://doi.org/10.1186/s12859-015-0707-9>
- Ueno, H., J. Banchereau, and C.G. Vinuesa. 2015. Pathophysiology of T follicular helper cells in humans and mice. *Nat. Immunol.* 16:142–152. <https://doi.org/10.1038/ni.3054>
- Ulas, T., S. Pirr, B. Fehlhaber, M.S. Bickes, T.G. Loof, T. Vogl, L. Mellinger, A. S. Heinemann, J. Burgmann, J. Schöning, et al. 2017. S100-alarmin-induced innate immune programming protects newborn infants from sepsis. *Nat. Immunol.* 18:622–632. <https://doi.org/10.1038/ni.3745>
- Ulloa, L., and S. Tabibzadeh. 2001. Lefty inhibits receptor-regulated Smad phosphorylation induced by the activated transforming growth factor-beta receptor. *J. Biol. Chem.* 276:21397–21404. <https://doi.org/10.1074/jbc.M010783200>
- Vanders, R.L., P.G. Gibson, V.E. Murphy, and P.A. Wark. 2013. Plasmacytoid dendritic cells and CD8 T cells from pregnant women show altered phenotype and function following H1N1/09 infection. *J. Infect. Dis.* 208:1062–1070. <https://doi.org/10.1093/infdis/jit296>
- Yaari, G., C.R. Bolen, J. Thakar, and S.H. Kleinstein. 2013. Quantitative set analysis for gene expression: a method to quantify gene set differential expression including gene-gene correlations. *Nucleic Acids Res.* 41:e170. <https://doi.org/10.1093/nar/gkt660>
- Yockey, L.J., and A. Iwasaki. 2018. Interferons and proinflammatory cytokines in pregnancy and fetal development. *Immunity*. 49:397–412. <https://doi.org/10.1016/j.immuni.2018.07.017>
- Zeng, W., Z. Liu, S. Zhang, J. Ren, X. Ma, C. Qin, F. Tian, Y. Zhang, and Y. Lin. 2016. Characterization of T follicular helper cells in allogeneic normal pregnancy and PDL1 blockage-induced abortion. *Sci. Rep.* 6:36560. <https://doi.org/10.1038/srep36560>
- Zhao, L., R. He, H. Long, B. Guo, Q. Jia, D. Qin, S.Q. Liu, Z. Wang, T. Xiang, J. Zhang, et al. 2018. Late-stage tumors induce anemia and immunosuppressive extramedullary erythroid progenitor cells. *Nat. Med.* 24:1536–1544. <https://doi.org/10.1038/s41591-018-0205-5>